



Original Research

Application of Bayesian model and discriminant function analysis to the estimation of sediment source contributions

Pengfei Du ^a, Donghao Huang ^{b,*}, Duihu Ning ^a, Yuehong Chen ^a, Bing Liu ^a, Jian Wang ^a, Jingjing Xu ^a^a State Key Laboratory of Simulation and Regulation of Water Cycle in River Basin, China Institute of Water Resources and Hydropower Research, Beijing, 100048, China^b Faculty of Geographical Science, Beijing Normal University, Beijing, 100875, China

ARTICLE INFO

Article history:

Received 8 November 2018

Received in revised form

30 April 2019

Accepted 21 May 2019

Available online 7 June 2019

Keywords:

Sediment fingerprinting

Sediment source contribution

Walling-Collins model

Bayesian model

Discriminant function analysis

ABSTRACT

Bayesian and discriminant function analysis (DFA) models have recently been used as tools to estimate sediment source contributions. Unlike existing multivariate mixing models, the accuracy of these two models remains unclear. In the current study, four well-distinguished source samples were used to create artificial mixtures to test the performance of Bayesian and DFA models. These models were tested against the Walling-Collins model, a credible model used in estimation of sediment source contributions estimation, as a reference. The artificial mixtures were divided into five groups, with each group consisting of five samples with known source percentages. The relative contributions of the sediment sources to the individual and grouped samples were calculated using each of the models. The mean absolute error (MAE) and standard error of (SE) MAE were used to test the accuracy of each model and the robustness of the optimized solutions. For the individual sediment samples, the calculated source contributions obtained with the Bayesian (MAE = 7.4%, SE = 0.6%) and Walling-Collins (MAE = 7.5%, SE = 0.7%) models produced results which were closest to the actual percentages of the source contributions to the sediment mixtures. The DFA model produced the worst estimates (MAE = 18.4%, SE = 1.4%). For the grouped sediment samples, the Walling-Collins model (MAE = 5.4%) was the best predictor, closely followed by the Bayesian model (MAE = 5.9%). The results obtained with the DFA model were similar to the values for the individual sediment samples, with the accuracy of the source contribution value being the poorest obtained with any of the models (MAE = 18.5%). An increase in sample size improved the accuracies of the Walling-Collins and Bayesian models, but the DFA model produced similarly inaccurate results for both the individual and grouped sediment samples. Generally, the accuracy of the Walling-Collins and Bayesian models was similar ($p > 0.01$), while there were significant differences ($p < 0.01$) between the DFA model and the other models. This study demonstrated that the Bayesian model could provide a credible estimation of sediment source contributions and has great practical potential, while the accuracy of the DFA model still requires considerable improvement.

© 2019 International Research and Training Centre on Erosion and Sedimentation/the World Association for Sedimentation and Erosion Research. Published by Elsevier B.V. All rights reserved.

1. Introduction

Patterns formed by sediment dynamics in catchments and river systems provide important information on nutrient and contaminant redistribution, such as organic pollutants, which can lead to eutrophication, and heavy metals (e.g., Pimentel et al., 1995; Smith et al., 2011). Information on the contribution of sediment sources is useful for comprehensive catchment management. Sediment

fingerprinting provides an effective and convenient way to quantify sediment source information. Since the sediment source fingerprinting technique was first used in the 1970s, it has greatly advanced and become more widely used (Walling, 2013). To date, considerable progress has been made to improve sediment fingerprinting techniques and reduce the uncertainty that results from: the preselection of potential material sources (Collins et al., 2010; Liu et al., 2011; Minella et al., 2008; Rabesiranana et al., 2016; Walling et al., 1993), sampling strategies (Davis & Fox, 2009; Du & Walling, 2017; Gellis & Noe, 2013; Haddadchi et al., 2015; Wilkinson et al., 2013, 2015), and tracer selection (Blake et

* Corresponding author.

E-mail address: donghaohuang@mail.bnu.edu.cn (D. Huang).

al., 2012; Kimoto et al., 2006; McKinley et al., 2013; Sherriff et al., 2015; Zhang et al., 2001).

Estimation models have also received great attention, as they have allowed the contributions of different sediment sources to be determined by comparing sediment properties. However, clarification of the uncertainty and accuracy of these models is needed. The widely used Walling-Collins model developed by Walling et al. (1993) and Collins et al. (1997) has undergone continuous improvement, such as adding correction factors or weights to the model (Collins et al., 2010). However, addition of correction factors and weights has resulted in overcorrection in some situations, which may bias the estimated contribution results (Martinez-Carreras et al., 2008; Zhang & Liu, 2016). Since the introduction of the Walling-Collins model, several types of multivariate mixing models also have been proposed. Examples of these models include: the Hughes model, which aims at attaining the lowest error for individual samples but not the mean value when taking a

Monte Carlo approach (Hughes et al., 2009; Olley & Caitcheon, 2000); the Motha model, which illustrates uncertainties caused by variations in source and sediment tracer properties by minimizing the objective function and including an additional tolerance criterion for the goodness-of-fit (Motha et al., 2003); the Landwehr model, which applies a normalized standard deviation from multiple sources, which makes the statistics used in the model more powerful (Devereux et al., 2010); and the distribution model, which uses the Pearson correlation and incorporates Student's t-distribution for fingerprint properties and normal distribution for sediment into the modeling framework (Lacey & Olley, 2015).

For the foregoing multivariate mixing models and their modified versions, the principles of sediment source estimation are basically similar. They generate random values for the fingerprint properties using Latin Hypercube sampling strategies and obtain globally optimal solutions through the application of genetic algorithm optimization. However, the different models usually

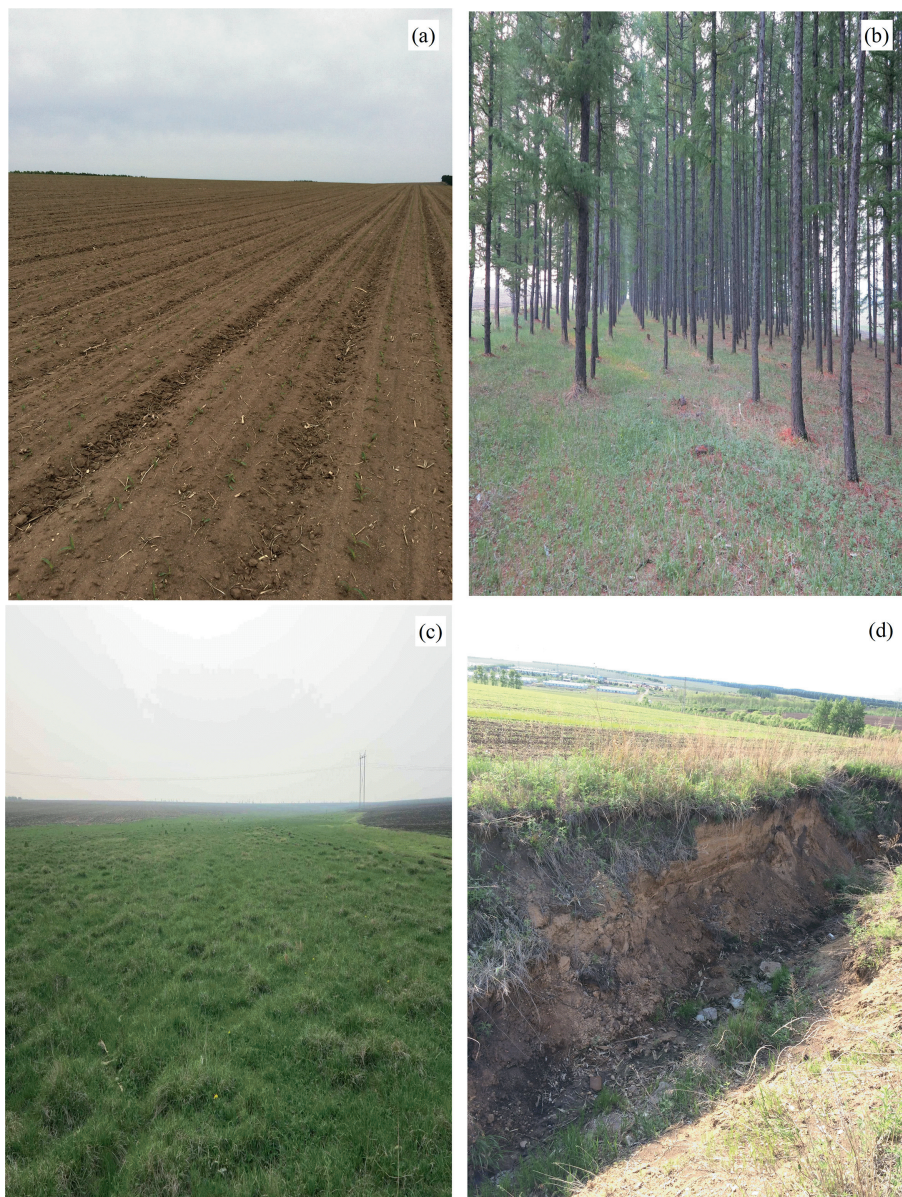


Fig. 1. Photographs of the four potential sediment source areas used in this study: (a) Cultivated land, (b) Forest, (c) Grassland, and (d) Gully banks.

generate different results and their assessment is important. Haddadchi et al. (2014) evaluated the representative multivariate mixing models. They showed that the predictor proposed by Laceby and Olley (2015) provided the most accurate estimates and the Walling-Collins model without weighting terms gave similar estimates. The modified model proposed by Collins Webb et al. (2010) with tracer discriminatory and within-source variability weights yielded the worst performance.

Other types of models that have been used to estimate sediment source contributions include Bayesian and discriminant function analysis (DFA) models. The Bayesian model incorporates uncertainty into the mixing models and makes full use of existing information (D'Haen et al., 2013; Moore & Semmens, 2008). Bayesian model was introduced quite early (Small & Rowan, 2002), but did not gain popularity until recently (D'Haen et al., 2013; Nosrati, 2017; Nosrati et al., 2014). DFA model can be used to quantify sediment source contributions while avoiding the use of mixing models altogether (Liu et al., 2016). The principles of operation of these two types of models are totally different from the multivariate mixing models.

There have been no assessments of Bayesian and DFA model performance in sediment source contribution studies. To test whether these models can be applied to the accurate estimation of sediment source contributions, artificial mixtures of four well-distinguished sources were prepared. As the Walling-Collins model without correction factors has proven effective (Haddadchi et al., 2014) and has been most widely used (Martinez-Carreras et al., 2008; Owens et al., 1999; Zhang & Liu, 2016), it was also applied in this assessment, as representative of multivariate mixing models. The results of the current research can provide an objective theoretical basis and avoid blind selection when estimating of potential sediment source contributions.

2. Material and methods

2.1. Artificial mixtures

Samples were collected from a small sub-basin of the Hebei catchment (49°01'20"N, 125°18'46"E), in the black soil region of Heilongjiang Province, northeast China. Cultivated land, forests, grassland, and gully banks were identified as being the main sediment source areas in this catchment (Fig. 1). Five samples were collected from each source area, giving a total of 20 samples. Topsoil samples from the cultivated land, forest, and grassland source areas were collected from a depth of 0–5 cm using a steel ring (7.5 cm diameter and 5.0 cm high). To increase the representativeness of the individual samples, three subsamples were collected within a radius of about 2 m at each site. The gully samples were composite samples collected from the full vertical profile of the gully side with particular focus on the B and C horizons (illuvial horizon and parent material horizon). To limit particle size effects, samples were passed through a 63- μ m sieve. Five different artificial mixture groups were created based on the weight of randomly selected samples collected from each source, with each group consisting of five artificial samples (Fig. 2).

Group 1 Identical amounts (9 g) of randomly selected samples from each source type were mixed to make five artificial sediment samples (M1–M5). Each of the source types each made a 25% contribution to the artificial samples.

Group 2 Identical amounts (9 g) of randomly selected samples from the forest, grassland, and gully bank areas were mixed with 3 g of the sample from cultivated land to make five artificial sediment samples (M6–M10). The cultivated land area sample contributed 10% of the artificial samples, and the other source area samples each contributed 30%.

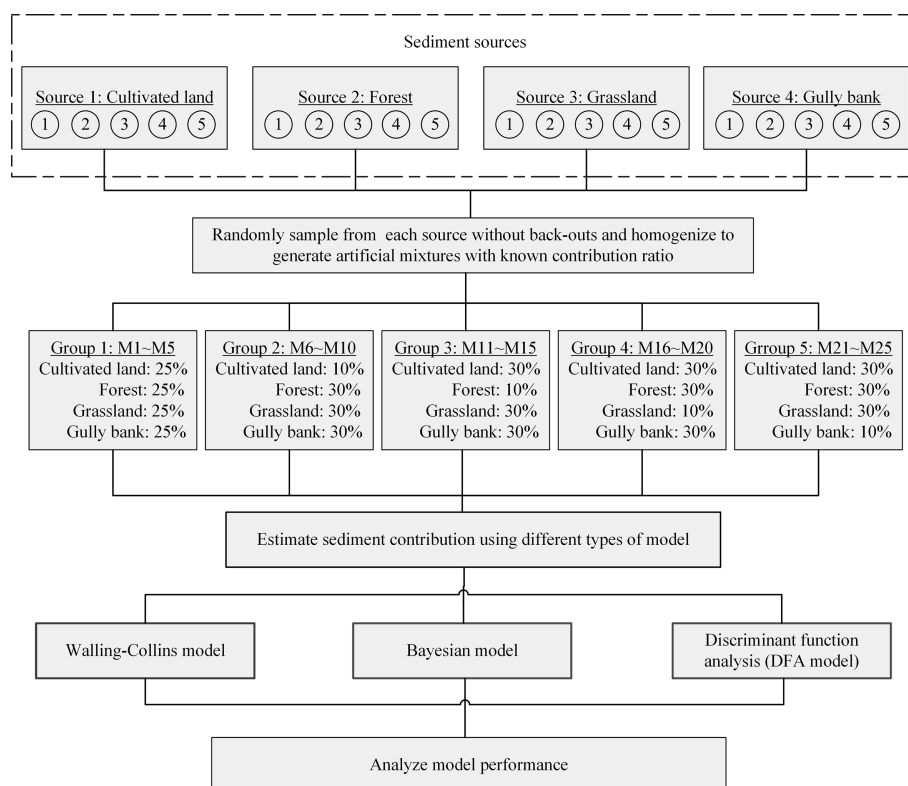


Fig. 2. Flow chart outlining the process used to test model accuracy given source proportion of artificially made sediments.

- Group 3 Identical amounts (9 g) of randomly selected samples from cultivated land, grassland, and gully bank areas were mixed with 3 g of the sample from the forest area to make five artificial sediment samples (M11–M15). The forest area sample contributed 10% of the five artificial samples, and the other source area samples each contributed 30%.
- Group 4 Identical amounts (9 g) of randomly selected samples from the cultivated land, forest, and gully bank areas were mixed with 3 g of the sample from the grassland area to make five artificial sediment samples (M16–M20). The grassland area sample contributed 10% of the artificial samples, and the other source area samples each contributed 30%.
- Group 5 Identical amounts (9 g) of randomly selected samples from the cultivated land, forest, and grassland areas were mixed with 3 g of the sample from the gully bank area to make five artificial sediment samples (M21–M25). The gully bank sample contributed 10% of the artificial samples and the other source area samples each contributed 30%.

2.2. Tracer properties analysis

Inorganic nutrient, trace metal, heavy metal, and rare earth element content in the source and artificial sediment samples were analyzed by X-ray fluorescence spectrometry. In total, 29 chemical elements were identified, namely, phosphorus (P), titanium (Ti), vanadium (V), chromium (Cr), manganese (Mn), cobalt (Co), nickel (Ni), copper (Cu), zinc (Zn), gallium (Ga), arsenic (As), bromine (Br), rubidium (Rb), strontium (Sr), yttrium (Y), zirconium (Zr), niobium (Nb), barium (Ba), lanthanum (La), cerium (Ce), neodymium (Nd), lead (Pb), silicon dioxide (SiO₂), aluminum oxide (Al₂O₃), iron oxide (Fe₂O₃), magnesium oxide (MgO), calcium oxide (CaO), potassium oxide (K₂O), and sodium oxide (Na₂O).

2.3. Sediment fingerprinting models

Based on the evaluation of Haddadchi et al. (2014), the Walling-Collins model without weighting terms offers a high level of accuracy. In view of its common use, this model was selected for comparison with the Bayesian and DFA models. All three models were coded in Matlab.

2.3.1. Walling-Collins model

The algorithm used by Walling et al. (1993) and Collins et al. (1997) was used for this evaluation. To minimize the error term, the algorithm was expressed as follows:

$$E = \sum_{i=1}^m \left\{ \left[C_i - \left(\sum_{s=1}^n P_s S_{si} \right) / C_i \right]^2 \right\} \quad (1)$$

assuming:

$$0 \leq P_s \leq 1 \quad (2)$$

$$\sum_{s=1}^n P_s = 1 \quad (3)$$

where m is the number of potential sediment sources, C_i is the concentration of the i th fingerprint property in the sediment sample, n is the number of fingerprint properties, P_s is the percentage contribution of sediment source s , and S_{si} is the concentration of fingerprint property i in sediment source sample s . The mean and standard deviation of the fingerprint properties were

used to do random repeat sampling 2500 times with the Latin Hypercube sampling method (LHS) and genetic algorithm (GA) optimization (Collins et al., 2012).

2.3.2. Bayesian model

The Bayesian model was originally used in predator–prey case studies to assess the contributions of different sources (Preys) to a mixture (Consumer) in ecology (Moore & Semmens, 2008). The model was used to quantify uncertainty by calculating the probability distributions for the proportional contribution f_i of each source i to the mixture of the four sources. According to the Bayes rule, the post probability of each f_q is calculated based on the data and prior information, as follows:

$$P(f_q | data) = \frac{L(data|f_q) \times p(f_q)}{\sum L(data|f_q) \times p(f_q)} \quad (4)$$

where $L(data|f_q)$ is the likelihood of the data, given that f_q , $p(f_q)$ represents the prior probability of the given state being true based on prior information, and f_q is the proportional source contribution of q proposed vectors.

The likelihood of this distribution is then determined by calculating the product of the likelihood of each individual mixture tracer value, given the proposed mixture distribution specific to that tracer. The proposed tracer distributions for the mixture are determined by solving for the proposed means $\hat{\mu}_j$ and standard deviations $\hat{\sigma}_j$ of the mixture based on the randomly drawn f_i values constituting the vector f_q . Once the values of $\hat{\mu}_j$ and $\hat{\sigma}_j$ are determined, the likelihood of the data given the proposed mixture is calculated as:

$$L(x | \hat{\mu}_j, \hat{\sigma}_j) = \prod_{k=1}^n \prod_{j=1}^n \left\{ \frac{1}{\hat{\sigma}_j \times \sqrt{2} \times \pi} \times \exp \left[-\frac{(x_{kj} - \hat{\mu}_j)^2}{2 \times \hat{\sigma}_j^2} \right] \right\} \quad (5)$$

where x_{kj} is the j th tracer property of the k th sediment sample. The sampling-importance-resampling algorithm (Rubin, 1988) was used to generate samples from the posterior distribution of the estimated mixture.

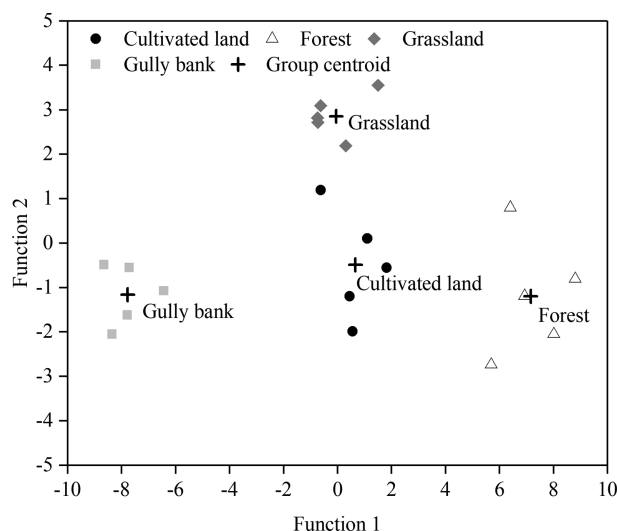


Fig. 3. Scatterplot of first and second discriminant functions calculated using stepwise DFA associated selection of the optimum composite fingerprint.

2.3.3. Discriminant function analysis (DFA) model

DFA is a standard procedure for optimized composite fingerprint selection. Liu et al. (2016) recognized that the DFA output could be used to directly quantify the source contribution without any extra procedures in the mixing models, as follows:

$$D_m = \sum_{i=1}^f \frac{\rho_i}{100} |F_i(\text{source}_m) - F_i(\text{sediment})| \quad (6)$$

$$W_m = 1/D_m \quad (7)$$

$$W = \sum_{i=1}^m 1/D_m \quad (8)$$

$$P_m = (W_m/W) \times 100 \quad (9)$$

where D_m is the distance from source m , ρ_i is the rate (%) of F_i to classify sources, F_i is the discriminant function obtained from the DFA output, f is the number of discriminant functions, W_m is the weighting for source m , W is the total weighting, P_m is the contribution of source m (%), $F_i(\text{source}_m)$ and $F_i(\text{sediment})$ are the centers of the source m and sediment based on the function i , respectively. A scatter plot of the first and second discriminant functions determined from stepwise DFA of the four potential sediment sources and artificial sediment samples is shown in Fig. 3.

2.4. Accuracy of models

The mean absolute error (MAE) was used to test the accuracy of each model as follows:

$$\text{MAE} = \frac{\sum_{j=1}^m |AP_j - CP_j|}{m} \quad (10)$$

where AP_j is the actual percentage of source j in the artificial mixtures, CP_j is the calculated percentage of source j , and m is the number of sources.

3. Results

3.1. Characteristics of the fingerprinting tracers

The 25 studied sediment samples were created artificially and underwent no mobilization or transport. Therefore, the tracer concentrations of each sample were bounded by a quadrangle formed by the average concentrations of the four source samples. All tracers broadly passed the bracket test. The Kruskal–Wallis hypothesis test (H-test), a nonparametric procedure, was used to select tracers that exhibited significant differences between the potential sediment sources (Liu et al., 2016). The H-test revealed that the P, Ti, V, Cr, Mn, Cu, Ga, Br, Y, Zr, Nb, Ba, Nd, SiO₂, Al₂O₃, CaO, K₂O, and Na₂O contents were significantly different for the four potential sources at the $p < 0.05$ (Table 1).

DFA has conventionally been used to identify important dimensions and minimize the number of tracers to those that best allow discrimination between sources. The 18 tracers that passed the H-test were analyzed by DFA, and the tracers Al₂O₃, Br, Ba, P, and SiO₂ passed the DFA procedure as the optimum composite fingerprint. This tracer selection correctly classified 95.0% of the original grouped samples (Table 2). Fig. 3 shows a scatterplot of the first and second discriminant functions which separates the cultivated land, forest, grassland, and gully bank areas based on the final

Table 1

Output resulting from application of the Kruskal–Wallis H-test to the source-type fingerprint property data that passed dual-range bracket testing for the studied catchment.

Fingerprinting tracers		H-value	p-value
1	P	14.943	0.002
2	Ti	12.243	0.007
3	V	12.884	0.005
4	Cr	10.391	0.016
5	Mn	9.933	0.019
6	Co	3.231	0.357*
7	Ni	4.310	0.230*
8	Cu	8.881	0.031
9	Zn	5.049	0.168*
10	Ga	11.216	0.011
11	Br	11.824	0.008
12	As	7.345	0.062*
13	Rb	7.383	0.061*
14	Sr	7.051	0.070*
15	Y	11.280	0.010
16	Zr	8.057	0.045
17	Nb	9.353	0.025
18	Ba	10.528	0.015
19	La	1.907	0.592*
20	Ce	3.397	0.334*
21	Nd	10.300	0.016
22	Pb	6.889	0.076*
23	SiO ₂	13.223	0.004
24	Al ₂ O ₃	16.429	0.001
25	Fe ₂ O ₃	5.565	0.135*
26	CaO	10.622	0.014
27	MgO	4.104	0.250*
28	K ₂ O	9.609	0.022
29	Na ₂ O	8.206	0.042

*Not significantly different at $p < 0.05$ level.

Table 2

Optimum composite fingerprints for discrimination of sediment source types in the studied catchment.

Step	Variable	Correctly classified cumulative source type sample (%)	Correctly classified source-type sample (%)	p-level
1	Al ₂ O ₃	80.0	80.0	<0.05
2	Br	83.5	55.5	<0.05
3	Ba	90.0	60.0	<0.05
4	P	92.8	55.0	<0.05
5	SiO ₂	95.0	65.0	<0.05

composite fingerprint. The mean, standard variation, and correlation coefficients for optimum composite fingerprints for the four sediment sources are listed in Tables 3 and 4.

Concentration data and probability distributions of the optimum composite fingerprint used to discriminate between cultivated land, forest, grassland, and gully bank areas are shown in Fig. 4. Based on the scatterplot in Fig. 3, the cultivated land samples are relatively discrete and best correspond to that of grassland. The centroid distance between the cultivated land and grassland areas is the shortest, which leads to a large overlap area in the probability distributions of these two sources (Fig. 4). This is because the grassland area is located at the foot of sloping land and is greatly affected by sediment eroded from cultivated land on the slope. However, grassland and cultivated land still were significantly different and separated as different sediment sources. In contrast, data from the gully bank samples were clearly distinguished from those taken from the other sources (Fig. 3). The probability distributions of the fingerprinting tracers from the gully bank samples in Fig. 4 clearly are separate from cultivated land, forest, and grassland distributions, with the exception of Ba.

Table 3

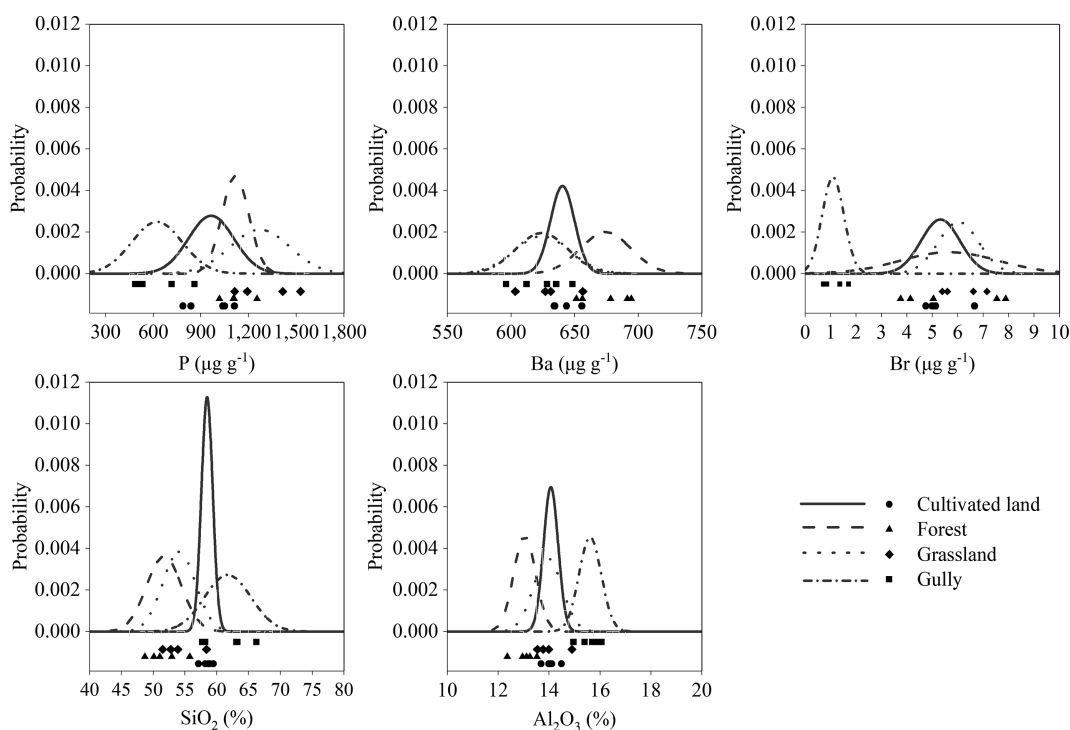
Mean, coefficient of variance (CV), and standard deviation (SD) of tracers that passed DFA for the studied land use types.

Land use types		Sediment fingerprinting tracers					Sample size
		P	Br	Ba	SiO ₂	Al ₂ O ₃	
		μg/g	μg/g	μg/g	%	%	
Cultivated land	Mean	964.3	5.32	640.42	58.46	14.07	5
	SD	143.07	0.79	9.45	0.89	0.29	
	CV	0.148	0.148	0.015	0.015	0.021	
Forest	Mean	1,116.88	5.66	674.38	51.7	13.04	5
	SD	84.79	1.92	19.87	2.74	0.44	
	CV	0.076	0.339	0.029	0.053	0.034	
Grassland	Mean	1,271.12	6.02	624.28	54.06	13.94	5
	SD	188.75	0.78	22.13	2.6	0.56	
	CV	0.148	0.130	0.035	0.048	0.040	
Gully bank	Mean	623.54	1.1	624.2	61.71	15.61	5
	SD	160.03	0.43	20.33	3.65	0.44	
	CV	0.257	0.391	0.033	0.059	0.028	

Table 4

Correlation coefficients for selected tracers for the four sediment sources.

Tracers	P	Br	Ba	SiO ₂	Al ₂ O ₃	P	Br	Ba	SiO ₂	Al ₂ O ₃
<i>Cultivated land</i>					<i>Forest</i>					
P	1					1				
Br	0.153	1				0.619	1			
Ba	0.043	-0.502	1			-0.770	-0.874	1		
SiO ₂	-0.450	0.226	0.080	1		-0.633	-0.849	0.769	1	
Al ₂ O ₃	-0.556	0.153	-0.391	-0.347	1	-0.105	0.203	0.146	0.206	1
<i>Grassland</i>					<i>Gully bank</i>					
P	1					1				
Br	0.998 ^b	1				-0.738	1			
Ba	0.935 ^a	0.918 ^a	1			0.842	-0.805	1		
SiO ₂	0.458	0.488	0.545	1		0.839	-0.883 ^a	0.962 ^b	1	
Al ₂ O ₃	0.807	0.801	0.931 ^a	0.796	1	-0.743	0.741	-0.533	-0.520	1

^a Correlation is significant at the 0.05 level.^b Correlation is significant at the 0.01 level.**Fig. 4.** Concentration plots of source samples and the probability distributions of P, Ba, Br, SiO₂, and Al₂O₃ for the four sediment source areas.

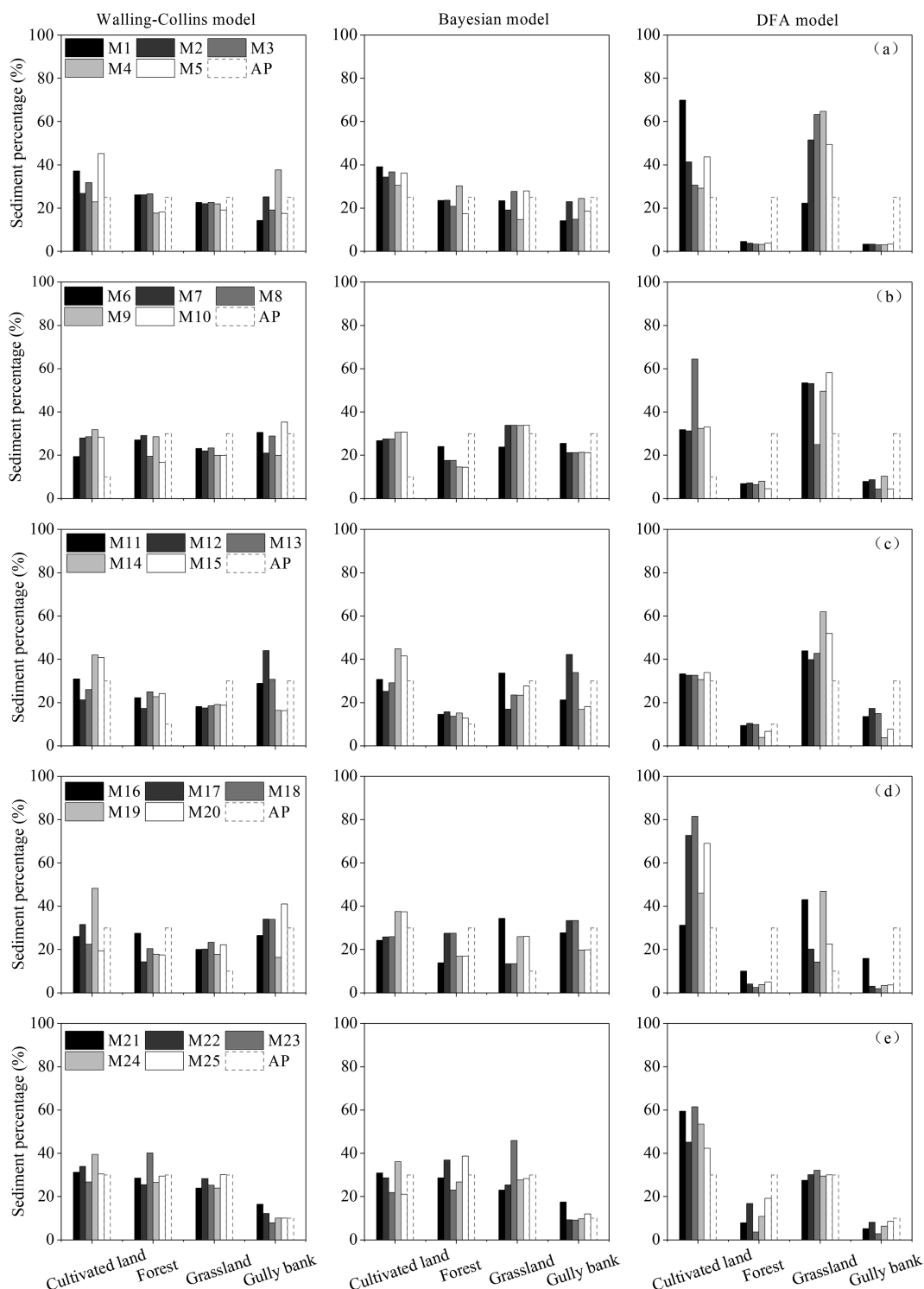


Fig. 5. Results of the Walling-Collins, Bayesian, and DFA sediment fingerprinting models of the individual sediment samples. AP is the actual percentage of each type of sediment in the mixed sediment.

3.2. Individual sediment samples

The contributions of each source in the twenty-five individual sediment samples (M1–M25) were calculated using the Walling-Collins, Bayesian, and DFA models. Fig. 5a shows the results obtained from each model for the Group 1 sediment samples (M1–M5: equal contribution from sources). Comparisons of these results, with the percentages for actual sediment samples

(dashed line) were based on mean absolute error (MAE) and average MAE (\overline{MAE}). The Walling-Collins model ($\overline{MAE} = 5.7\%$, SD. MAE = 3.2%) was the best model, followed by the Bayesian model ($\overline{MAE} = 6.3\%$, SD. MAE = 1.2%), and the DFA model ($\overline{MAE} = 21.8\%$, SD. MAE = 0.4%) exhibited the worst performance (Table 5).

The results for individual sediment samples from Group 2 (M6–M10; Fig. 5b: cultivated land = 10%, forest = 30%,

Table 5
Average mean absolute error ($\overline{\text{MAE}}$) and standard variation of MAE (SD. MAE) of the five artificial sediment samples in each group.

Artificial mixture sediments		Walling-Collins model	Bayesian model	DFA model
M1-M5	$\overline{\text{MAE}}$ (%)	5.7	6.3	21.8
	SD. MAE (%)	3.2	1.2	0.4
M6-M10	$\overline{\text{MAE}}$ (%)	9.2	10.8	23.7
	SD. MAE (%)	2.6	1.6	2.6
M11-M15	$\overline{\text{MAE}}$ (%)	10.0	6.8	10.3
	SD. MAE (%)	2.7	2.7	4.1
M16-M20	$\overline{\text{MAE}}$ (%)	9.2	8.5	24.7
	SD. MAE (%)	3.1	4.7	4.3
M21-M25	$\overline{\text{MAE}}$ (%)	3.4	4.8	11.4
	SD. MAE (%)	1.9	2.0	4.5

grassland = 30%, gully bank = 30%) indicated that the Walling-Collins model ($\overline{\text{MAE}} = 9.2\%$, SD. MAE = 2.6%) performed the best. This was followed by the Bayesian model ($\overline{\text{MAE}} = 10.8\%$, SD. MAE = 1.6%) and the DFA model ($\overline{\text{MAE}} = 23.7\%$, SD. MAE = 2.6%).

For the Group 3 samples (M11–M15; Fig. 5c: cultivated land = 30%, forest = 10%, grassland = 30%, gully bank = 30%) the Bayesian model produced results with the highest accuracy ($\overline{\text{MAE}} = 6.8\%$, SD. MAE = 2.7%). This was followed by the Walling-Collins model ($\overline{\text{MAE}} = 10.0\%$, SD. MAE = 2.7%), while the DFA model ($\overline{\text{MAE}} = 10.3\%$, SD. MAE = 4.1%) produced the poorest results.

Fig. 5d shows the results obtained for the Group 4 samples (M16–M20: cultivated land = 30%, forest = 30%, grassland = 10%, gully bank = 30%). Results obtained from the Bayesian model ($\overline{\text{MAE}} = 8.5\%$, SD. MAE = 4.7%) were closest to the actual sediment percentage from each source. This was followed by the Walling-Collins model ($\overline{\text{MAE}} = 9.2\%$, SD. MAE = 3.1%), while the results from the DFA model ($\overline{\text{MAE}} = 24.7\%$, SD. MAE = 4.3%) exhibited the worst performance.

Fig. 5e shows the results obtained for the Group 5 sample (M21–M25: cultivated land = 30%, forest = 30%, grassland = 30%, and gully bank = 10%). The Walling-Collins model ($\overline{\text{MAE}} = 3.4\%$, SD. MAE = 1.9%) produced the best prediction, followed by the Bayesian model ($\overline{\text{MAE}} = 4.8\%$, SD. MAE = 2.0%) and the DFA model ($\overline{\text{MAE}} = 11.4\%$, SD. MAE = 4.5%).

3.3. Groups of sediment samples

For Group 1, with equal contribution from each source the Walling-Collins model (MAE = 3.9%) performed best with an estimated 32.7% contribution from cultivated land, 23.5% from forest, 21.5% from grassland, and 22.4% from gully bank. The accuracy of the results produced by the Bayesian model (MAE = 9.4%) was much lower with an estimated 43.8% contribution from cultivated land, 22.3% from forest, 17.0% from grassland, and 11.6% from gully bank sources. The DFA model (MAE = 21.4%) exhibited the poorest performance with an estimated 49.8% contribution from cultivated land, 3.8% from forest, 43.1% from grassland, and 3.3% from gully bank sources (Fig. 6a; Table 6).

Fig. 6b shows the results obtained for Group 2 (cultivated land = 10%, forest = 30%, grassland = 30%, gully bank = 30%). These indicate that the Walling-Collins model (MAE = 9.1%) performed best with contributions of 28.2, 24.2, 21.2, and 26.5% from cultivated land, forest, grassland, and gully bank sources, respectively. The Bayesian model (MAE = 10.2%) exhibited a similar level of accuracy to that of the Walling-Collins model with 30.5, 22.0, 22.1, and 25.4% contributions from cultivated land, forest, grassland, and gully bank sources, respectively. The DFA model produced the

poorest results with a MAE of 24.9% (cultivated land = 30.7%, forest = 5.1%, grassland = 59.0%, gully bank = 5.2%).

For Group 3 (30% cultivated land, 10% forest, 30% grassland, and 30% gully bank), the Bayesian model proved to be the most accurate model with a MAE of 6.9%, and 43.0, 10.9, 20.6, and 25.6% contributions from cultivated land, forest, grassland, and gully bank sources, respectively. The Walling-Collins model was the next most accurate model with a MAE of 7.1% (cultivated land = 32.8%, forest = 21.4%, grassland = 18.7%, gully bank = 27.2%). The DFA model (MAE = 10.2%) was the most inaccurate model with 34.0, 8.5, 46.3, and 11.2% contributions from the cultivated land, forest, grassland, and gully bank, respectively (Fig. 6c).

For Group 4 (cultivated land = 30%, forest = 30%, grassland = 10%, gully bank 30%) the Bayesian model was the best predictor model with a MAE of 2.4% (cultivated land = 25.1%, forest = 30.8%, grassland = 13.5%, gully bank = 30.6%). The Walling-Collins model was the second-most accurate model with a MAE of 5.5% (cultivated land = 30.0%, forest = 19.1%, grassland = 21.0%, gully bank = 29.9%) while the DFA model (MAE = 26.5%) was the poorest model with 38.1, 3.7, 54.8, and 3.4% contributions from cultivated land, forest, grassland and gully bank, respectively (Fig. 6d).

For Group 5 (Fig. 6e; cultivated land = 30%, forest = 30%, grassland = 30%, gully bank = 10%) the Bayesian model (MAE = 0.4%) performed best (cultivated land = 30.2%, forest = 30.0%, grassland = 30.5%, gully bank = 9.3%). This was followed by the Walling-Collins model with a MAE of 1.7%. The DFA model (MAE = 11.1%) exhibited the poorest level of performance with 51.5, 11.2, 30.7, and 6.5% contributions from the cultivated land, forest, grassland, and gully bank, respectively.

4. Discussion

The principle on which the Bayesian model is based differs from that of the Walling-Collins model. The Bayesian model is based on probability theory. It makes full use of existing information and provides a priori estimates and uncertainties for the parameters according to the mean and variance ($\hat{\mu}_j, \hat{\sigma}_j$) of the prior distribution ($p(f_q)$), and then uses the observed data for different time points to estimate parameters. When a set of data is obtained, the posterior distribution obtained from the first set of data is taken as the a priori distribution. New data then are added to obtain the posterior distribution for the next step and the parameters are updated and estimated. In addition, the sampling-importance-resampling process extracts the samples from the important sampling function and does weighted sampling of the samples to make the samples approximate the objective function. Unlike the Bayesian model, the Walling-Collins model is an optimization calculation process. It is combined with the Latin hypercube sampling process to ensure estimation uniformity of the samples in space under the assumption that the fingerprint factor concentration in each sediment source exhibits a normal distribution. Global optimal solutions are calculated using a genetic algorithm.

To compare the uncertainty and accuracy associated with sediment fingerprinting, Figs. 7 and 8 show the frequency and posterior probability distributions of the proportional contributions estimated using the Walling-Collins and Bayesian models, respectively (the DFA model has no Monte Carlo sampling simulation or optimization calculation procedure). For the Walling-Collins model, the cultivated land source had the largest distribution range with an average standard deviation (ASD) of 24.0%. Because the forest and grassland are located at the backslope and toeslope of the cultivated land, respectively, soil eroded from the cultivated land tended to be deposited in the forest and grassland areas. This led to most of the tracer concentrations of these two sources being similar to that

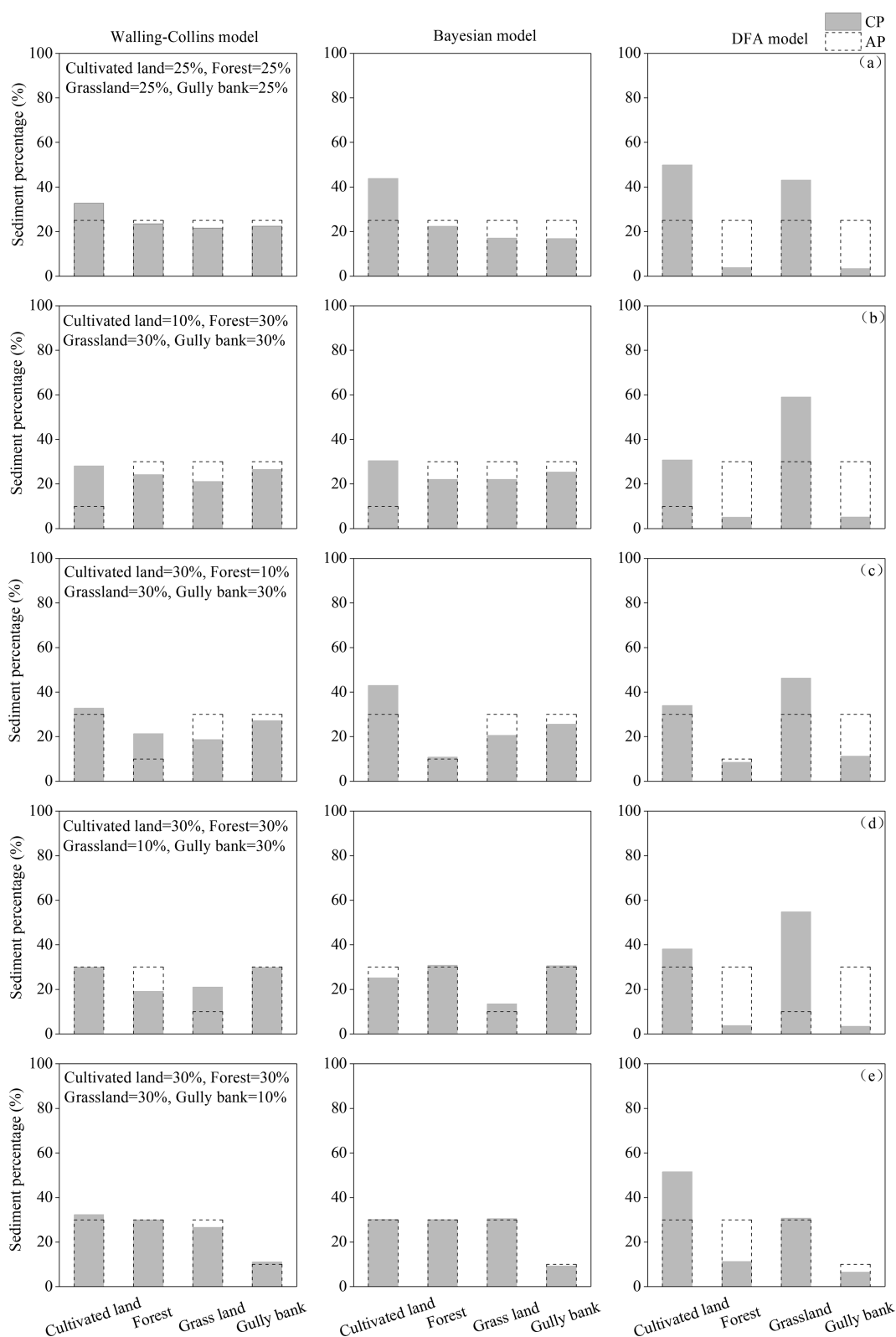


Fig. 6. Source contributions estimated by the Walling-Collins, Bayesian, and DFA models for the five categories of grouped sediment samples. AP is the actual percentage of each sediment source in the mixed sediment and CP is the calculated percentage of each source in the mixture.

of cultivated land (Table 3, Fig. 4). It is important to recognize that the actual amounts of sediment contributed by the different sources are distinct from their relative contributions. The relative contributions of sediment sources with similar tracer concentrations

interact, resulting in larger estimation ranges for forest (ASD = 16.0%) and grassland (ASD = 14.8%) sources, even though they are easy to distinguish from each other (Fig. 3). Unlike the forest and grassland samples, the gully bank samples represent the

Table 6
Mean absolute error (MAE) of the five artificial sediment groups.

Artificial mixture	Walling-Collins model	Bayesian model	DFA model
	MAE (%)		
Group 1	3.9	9.4	21.4
Group 2	9.1	10.2	24.9
Group 3	7.1	6.9	10.2
Group 4	5.5	2.4	26.5
Group 5	1.7	0.4	11.1

subsoil and are unaffected by other sources. The probability distributions of fingerprinting tracers from the gully bank areas were typically located in rightmost or leftmost positions on the charts

and exhibited minimal overlap with the other sources (Fig. 4). This results in the gully bank areas having the narrowest estimation distribution ranges ($ASD = 12.7\%$). To accurately estimate sediment source contributions and reduce uncertainty, the number of sediment sources needs to be minimized and sources with similar properties classified into one group. For example, the forest and grassland source areas of the current study could be combined into a single group.

The mathematical concepts of the Bayesian model differ from those of Walling-Collins model. The variation in the sediment source contributions was much more stable in the Bayesian model. As with the Walling-Collins model results, the distribution range of the cultivated land samples was widest with $ASD = 11.4\%$, followed by grassland, forest, and gully bank samples for which the ASD

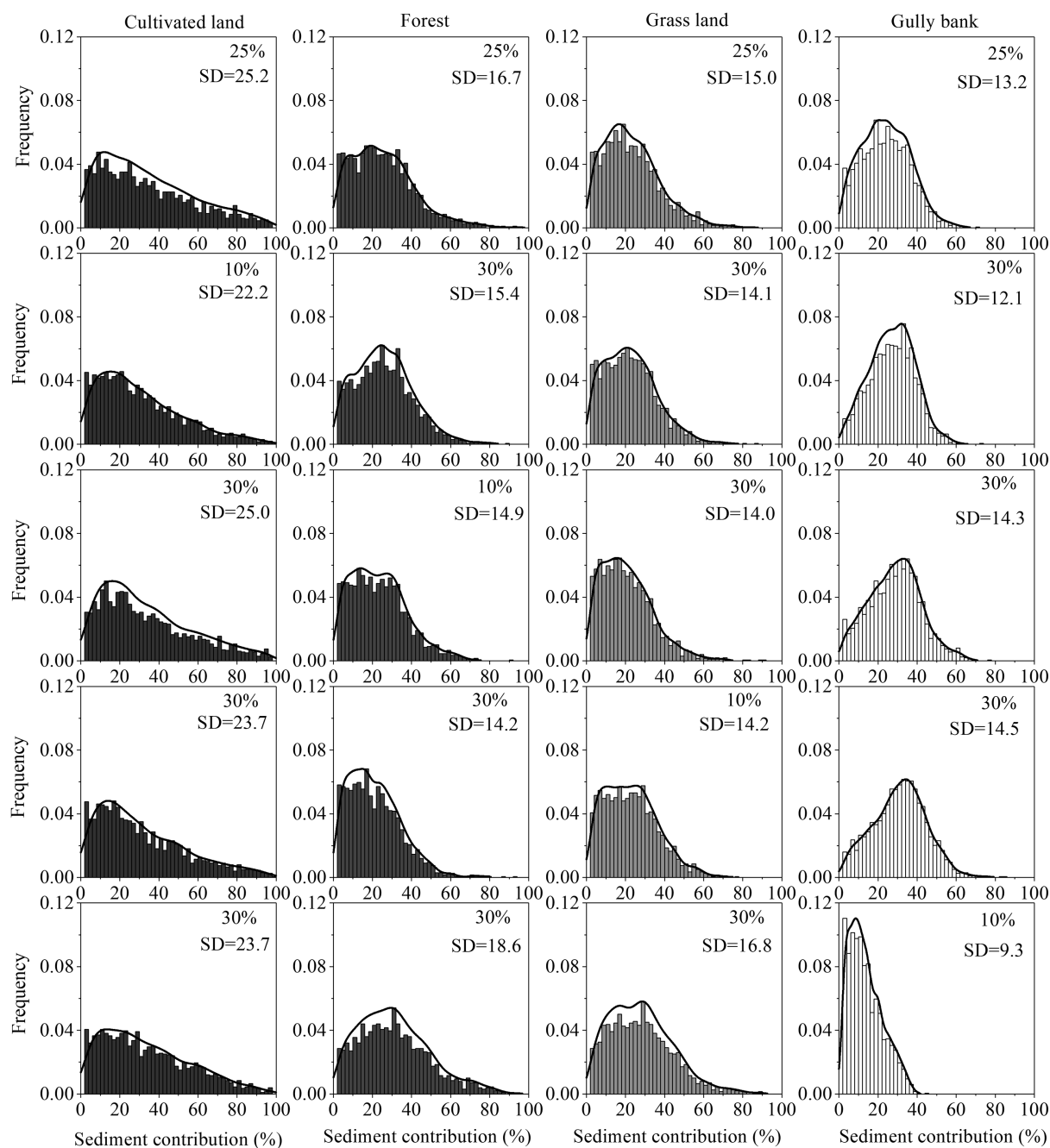


Fig. 7. Frequency distributions with standard deviation (SD) of the mean proportional contributions estimated using the Walling-Collins model.

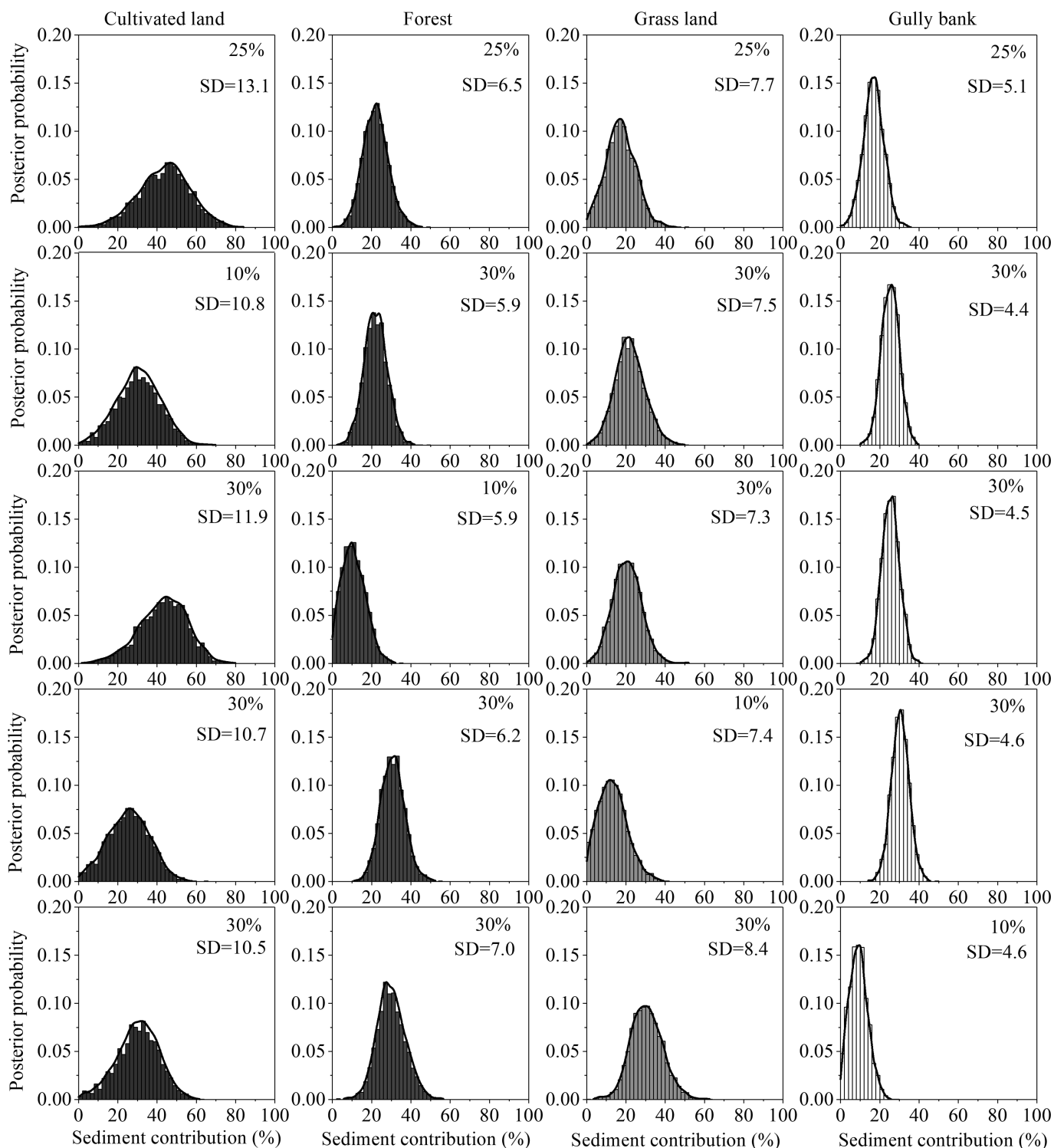


Fig. 8. Posterior probability distributions with standard deviation (SD) of the mean proportional contributions estimated using the Bayesian model.

Table 7

Performance of the three models using individual sediment samples and grouped sediment samples.

Estimation model	25 individual sediment samples (%)		Grouped sediment samples (%)	
	Average MAE	Standard error of MAE	Average MAE	Standard error of MAE
Bayesian	7.4	0.6	5.9	1.9
Walling-Collins	7.5	0.7	5.4	1.3
DFA	18.4	1.4	18.5	3.4

Table 8

The paired Student's t-test of MAE for the Walling-Collins, Bayesian, and DFA models.

Pairs		25 individual sediment samples		Grouped sediment samples	
		t-value	P-value	t-value	P-value
Pair 1	Walling-Collins & Bayesian	0.113	0.911	-0.276	0.796
Pair 2	Walling-Collins & DFA	-8.041	0.000	-4.200	0.014
Pair 3	Bayesian & DFA	-8.350	0.000	-3.851	0.018

Table 9

Tracer pairs subjected to discriminant function analysis and their abilities to discriminate between the four sediment sources.

No.	Tracer pairs			Discrimination ability
1	P	Br	Ba	95%
2	P	Br	SiO ₂	80%
3	P	Br	Al ₂ O ₃	80%
4	Br	Ba	SiO ₂	95%
5	Br	Ba	Al ₂ O ₃	90%
6	Ba	SiO ₂	Al ₂ O ₃	95%
7	P	Ba	SiO ₂	100%
8	P	Ba	Al ₂ O ₃	100%
9	P	SiO ₂	Al ₂ O ₃	85%
10	Br	SiO ₂	Al ₂ O ₃	80%

value was 7.7, 6.3, and 4.6%, respectively. Table 7 lists the performance and rankings of the models when applied to individual sediment samples and grouped sediment samples. For the individual sediment samples, the range of variation in the Bayesian

model results is within the range of the Walling-Collins model results. In general, the Bayesian model performed best with an average MAE for all samples being 7.4% with a standard error of 0.6%. The accuracy of the Walling-Collins model was similar to that of the Bayesian model with an average MAE of 7.5% and standard error of 0.7%, thus, indicating accurate results. The DFA model on the other hand, is almost incapable of producing satisfactory results for individual sediment samples, exhibiting an average MAE of 18.4% and a standard error of 1.4%. For the grouped sediment samples, the Walling-Collins model was best with an average MAE of 5.4% and a standard error of 1.3%. The Bayesian model was the next most accurate with an average MAE of 5.9% and a standard error of 1.9%. As with the individual sediment samples, the DFA model was unable to correctly predict the source contributions of the grouped sediment samples, having an average MAE of 18.5% and a standard error of 3.4%.

The accuracies of the estimations of the relative sediment source contributions, as provided by the Walling-Collins model and Bayesian model are similar ($p > 0.01$) for both individual and grouped sediment samples, and can be used interchangeably (Table 8). The outputs of the grouped sediment samples were found to be much higher than those for the individual sediment samples. This indicates that the composite samples consist of several sub-samples, which was done to enhance the representativeness of the sampled area. This sample-collection strategy was proven to provide an effective means of reducing random variability in the properties (Wilkinson et al., 2013). For the Bayesian model, increasing the number of samples provides more a priori information yielding more accurate source contribution estimates. Therefore, increasing the

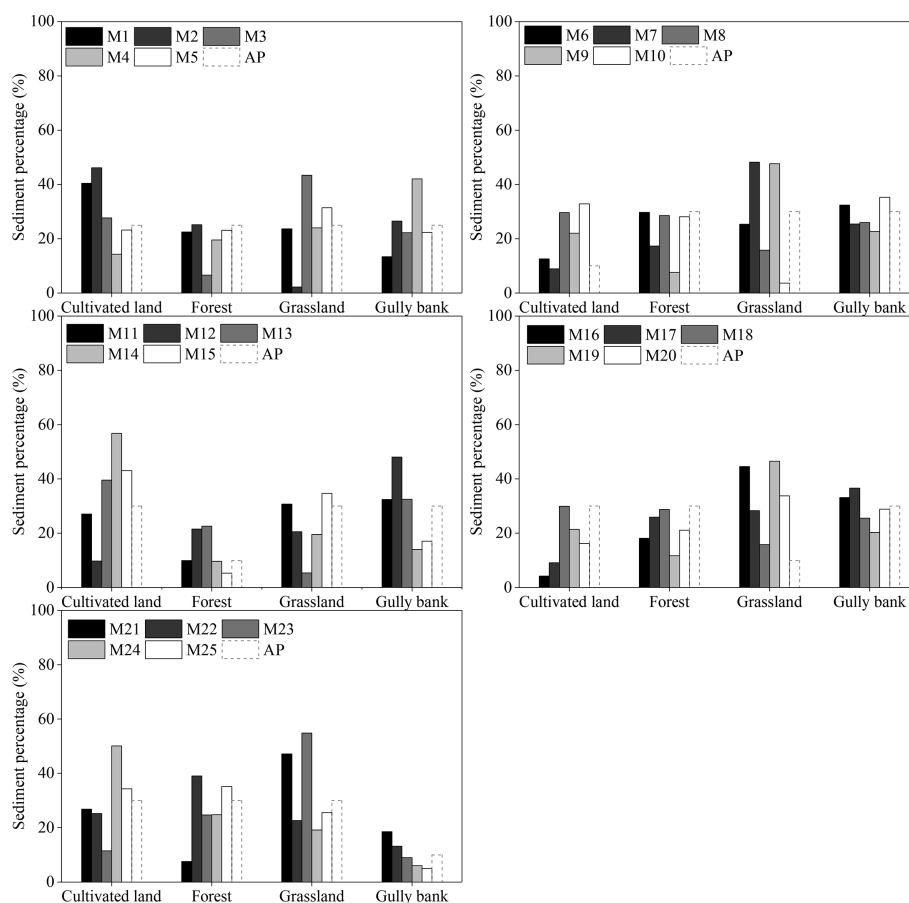


Fig. 9. Source contribution results of the analytical solution with tracer pairs in the individual sediment samples. AP is the actual percentage of each sediment in the mixed sediment.

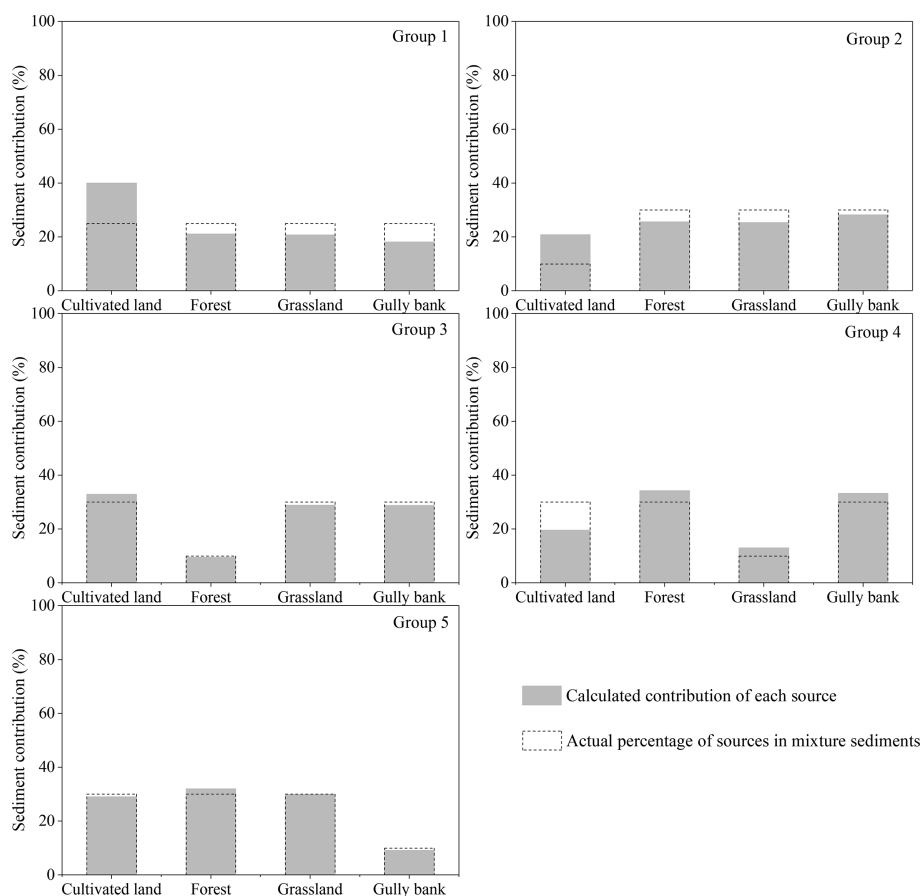


Fig. 10. Source contribution results for the analytical solution with tracer pairs in five categories of grouped sediment samples.

number of samples will improve the estimation results. Compared to the Walling–Collins and Bayesian models, the DFA model performed poorly when applied to both the individual and grouped sediment samples. The accuracy of DFA model and the other models was significantly different ($p < 0.01$; Table 8). Variations in the tracer concentration of a source within a group or between groups, and the types and number of tracers, all affect the centroid position and influence DFA model uncertainty. The DFA model does not apply the tracer concentrations directly, but builds functions that group sediment sources, and then infers the sediment contributions based on the distance from the source centroid to the sample. The DFA model reduces the uncertainty that arises from the different tracer concentration patterns (Liu et al., 2016). However, it can also lead to false recognition, as using either individual or grouped sediment samples produces similar results.

Zhang and Liu (2016) made full use of tracer information in the form of multiple composite fingerprints and tracer pairs to derive an analytical solution with tracers that had passed the H-test. However, their method involves high amounts of calculation. In the current study, the sediment contribution was estimated with tracer pairs that consisted of the final optimum composite fingerprints (P, Br, Ba, SiO₂, and Al₂O₃). Three tracers are needed to obtain analytical solutions for the four sediment sources and 10 ($C_n^{m-1} = C_5^3$) possible tracer pairs were produced (Table 9). For individual sediment samples, the mean concentration of each tracer in the source samples was used to calculate the sediment contributions to the 25 sediment sources. Negative solutions were eliminated, and the final proportion was the average of solutions calculated from tracer pairs as well as the five grouped sediment samples. Figs. 9 and 10 show the results obtained for the source contributions of

the individual and grouped sediment samples, respectively. The performance obviously is better than that of the DFA model, with accuracies of 9.0% and 4.1% for the individual and grouped sediment samples, respectively. However, this approach depends to a great extent on property analysis accuracy and the conservativeness of the tracers. In the current study, the sediment samples were created artificially and had not undergone the erosion process including transport, movement, and sedimentation. The tracers exhibited almost no chemical change or dissolution between the source and the artificial sediment samples. Therefore, it is feasible to use this method for tracers that are environmentally stable.

5. Conclusions

The current study investigated the potential of the Bayesian model and DFA model for estimating sediment source contribution through the validation of artificial mixtures with well-distinguished sources. The performance of the two models also were compared against the Walling–Collins model, one of the most representative of the multivariate mixing models. The Bayesian model provided an estimation with a high level accuracy similar to that obtained with the Walling–Collins model. The DFA model, however, failed to perform satisfactorily when applied to sediment source estimation.

For individual sediment samples, the Bayesian model produced an estimate of the source contributions that was closer to the actual percentage than the other models. The Walling–Collins model was the second-most accurate model, and only slightly less accurate than the Bayesian model, whereas the difference between estimates provided by the DFA model and the actual values was much greater.

Regarding the prediction accuracy of the source contributions to the grouped sediment samples, the Walling–Collins and Bayesian models both performed well, and the DFA model results were less reliable. Compared with the individual sediment samples, the accuracy of the estimations of the sediment source relative contributions for the grouped sediment samples, as determined by the Walling–Collins and Bayesian models, were both much higher. This further reveals that increasing the number of sediment samples greatly improved the representativeness of the tracer concentrations. However, results produced by the DFA model were similar for the individual and grouped sediment samples, suggesting that there is still potential to improve this model. An analytical solution based on tracer pair proportions offers the potential to estimate sediment source contributions, especially for conservative tracers in a stable environment.

Acknowledgements

This work was supported by the National Key Research and Development Program [grant number 2016YFC0500802], the National Natural Science Foundation of China [grant number 41501299, 41701322], the special fund of State Key Laboratory of Simulation and Regulation of a Water Cycle in a River Basin, China Institute of Water Resources and Hydropower Research [grant number SKL2018TS08], and IWH Research & Development Support Program [grant number SC0145B172019].

Appendix A. Supplementary data

Supplementary data to this article can be found online at <https://doi.org/10.1016/j.ijsrc.2019.05.005>.

References

- Blake, W. H., Ficken, K. J., Taylor, P., Russell, M. A., & Walling, D. E. (2012). Tracing crop-specific sediment sources in agricultural catchments. *Geomorphology*, *139*–140, 322–329.
- Collins, A. L., Walling, D. E., & Leeks, G. J. L. (1997). Source type ascription for fluvial suspended sediment based on a quantitative composite fingerprinting technique. *Catena*, *29*, 1–27.
- Collins, A. L., Walling, D. E., Stroud, R. W., Robson, M., & Peet, L. M. (2010). Assessing damaged road verges as a suspended sediment source in the Hampshire Avon catchment, southern United Kingdom. *Hydrological Processes*, *24*(9), 1106–1122.
- Collins, A. L., Walling, D. E., Webb, L., & King, P. (2010). Apportioning catchment scale sediment sources using a modified composite fingerprinting technique incorporating property weightings and prior information. *Geoderma*, *155*(3–4), 249–261.
- Collins, A. L., Zhang, Y., Walling, D. E., Grenfell, S. E., Smith, P., Grischeff, J., et al. (2012). Quantifying fine-grained sediment sources in the river Axe catchment, southwest England: Application of a Monte Carlo numerical modelling framework incorporating local and genetic algorithm optimisation. *Hydrological Processes*, *26*(13), 1962–1983.
- D'Haen, K., Verstraeten, G., Dusar, B., Degryse, P., Haex, J., & Waelkens, M. (2013). Unravelling changing sediment sources in a Mediterranean mountain catchment: A Bayesian fingerprinting approach. *Hydrological Processes*, *27*(6).
- Davis, C. M., & Fox, J. F. (2009). Sediment fingerprinting: Review of the method and future improvements for allocating nonpoint source pollution. *Journal of Environmental Engineering*, *135*(7), 490–504.
- Devereux, O. H., Prestegard, K. L., Needelman, B. A., & Gellis, A. C. (2010). Suspended-sediment sources in an urban watershed, northeast Branch Anacostia river, Maryland. *Hydrological Processes*, *24*(11), 1391–1403.
- Du, P., & Walling, D. E. (2017). Fingerprinting surficial sediment sources: Exploring some potential problems associated with the spatial variability of source material properties. *Journal of Environmental Management*, *194*, 4–15.
- Gellis, A. C., & Noe, G. B. (2013). Sediment source analysis in the Linganore Creek watershed, Maryland, USA, using the sediment fingerprinting approach: 2008 to 2010. *Journal of Soils and Sediments*, *13*(10), 1735–1753.
- Haddadchi, A., Olley, J., & Lacey, P. (2014). Accuracy of mixing models in predicting sediment source contributions. *The Science of the Total Environment*, *497*–498, 139–152.
- Haddadchi, A., Olley, J., & Pietsch, T. (2015). Quantifying sources of suspended sediment in three size fractions. *Journal of Soils and Sediments*, *15*(10), 2086–2100.
- Hughes, A. O., Olley, J. M., Croke, J. C., & McKergow, L. A. (2009). Sediment source changes over the last 250 years in a dry-tropical catchment, central Queensland, Australia. *Geomorphology*, *104*(3–4), 262–275.
- Kimoto, A., Nearing, M. A., Zhang, X. C., & Powell, D. M. (2006). Applicability of rare earth element oxides as a sediment tracer for coarse-textured soils. *Catena*, *65*(3), 214–221.
- Lacey, J. P., & Olley, J. (2015). An examination of geochemical modelling approaches to tracing sediment sources incorporating distribution mixing and elemental correlations. *Hydrological Processes*, *29*(6), 1669–1685.
- Liu, B., Storm, D. E., Zhang, X. J., Cao, W., & Duan, X. (2016). A new method for fingerprinting sediment source contributions using distances from discriminant function analysis. *Catena*, *147*, 32–39.
- Liu, G., Yang, M. Y., Warrington, D. N., Liu, P. L., & Tian, J. L. (2011). Using beryllium-7 to monitor the relative proportions of interrill and rill erosion from loessal soil slopes in a single rainfall event. *Earth Surface Processes and Landforms*, *36*(4), 439–448.
- Martinez-Carreras, N., Gallart, F., Iffly, J. F., Pfister, L., Walling, D. E., & Krein, A. (2008). Uncertainty assessment in suspended sediment fingerprinting based on tracer mixing models: A case study from Luxembourg. *Sediment Dynamics in Changing Environments*, *325*, 94–105.
- McKinley, R., Radcliffe, D., & Mukundan, R. (2013). A streamlined approach for sediment source fingerprinting in a Southern Piedmont watershed, USA. *Journal of Soils and Sediments*, *13*(10), 1754–1769.
- Minella, J. P. G., Walling, D. E., & Merten, G. H. (2008). Combining sediment source tracing techniques with traditional monitoring to assess the impact of improved land management on catchment sediment yields. *Journal of Hydrology*, *348*(3–4), 546–563.
- Moore, J. W., & Semmens, B. X. (2008). Incorporating uncertainty and prior information into stable isotope mixing models. *Ecology Letters*, *11*(5), 470–480.
- Motha, J. A., Wallbrink, P. J., Hairsine, P. B., & Grayson, R. B. (2003). Determining the sources of suspended sediment in a forested catchment in southeastern Australia. *Water Resources Research*, *39*(3), 1056.
- Nosrati, K. (2017). Ascribing soil erosion of hillslope components to river sediment yield. *Journal of Environmental Management*, *194*, 63–72.
- Nosrati, K., Govers, G., Semmens, B. X., & Ward, E. J. (2014). A mixing model to incorporate uncertainty in sediment fingerprinting. *Geoderma*, *217*–218, 173–180.
- Olley, J., & Caitcheon, G. (2000). Major element chemistry of sediments from the Darling–Barwon River and its tributaries: Implications for sediment and phosphorus sources. *Hydrological Processes*, *14*, 1159–1175.
- Owens, P. N., Walling, D. E., & Leeks, G. J. L. (1999). Use of floodplain sediment cores to investigate recent historical changes in overbank sedimentation rates and sediment sources in the catchment of the River Ouse, Yorkshire, UK. *Catena*, *36*, 21–47.
- Pimentel, D., Harvey, C., Resoudarmo, P., Sinclair, K., Kurz, D., McNair, M., & Blair, R. (1995). Environmental and economic costs of soil erosion and conservation benefits. *Science*, *267*, 1117–1123.
- Rabesrianana, N., Rasolonirina, M., Solonjara, A. F., Ravoson, H. N., Raelina, A., & Mabit, L. (2016). Assessment of soil redistribution rates by Cs-137 and Pbex-210 in a typical Malagasy agricultural field. *Journal of Environmental Radioactivity*, *152*, 112–118.
- Rubin, D. B. (1988). Using the SIR algorithm to simulate posterior distributions. *Bayesian statistics*, *3*, 395–402.
- Sherriff, S. C., Franks, S. W., Rowan, J. S., Fenton, O., & Ó'hUallacháin, D. (2015). Uncertainty-based assessment of tracer selection, tracer non-conservativeness and multiple solutions in sediment fingerprinting using synthetic and field data. *Journal of Soils and Sediments*, *15*(10), 2101–2116.
- Small, I. F., & Rowan, J. S. (2002). Quantitative sediment fingerprinting using a Bayesian uncertainty estimation framework. In F. J. Dyer, M. C. Thoms, & J. M. Olley (Eds.), *The structure, function and management implications of fluvial sedimentary systems* (pp. 443–450). Wallingford, UK: IAHS Press.
- Smith, H. G., Sheridan, G. J., Lane, P. N. J., Noske, P. J., & Heijnis, H. (2011). Changes to sediment sources following wildfire in a forested upland catchment, south-eastern Australia. *Hydrological Processes*, *25*(18), 2878–2889.
- Walling, D. E. (2013). The evolution of sediment source fingerprinting investigations in fluvial systems. *Journal of Soils and Sediments*, *13*(10), 1658–1675.
- Walling, D. E., Woodward, J. C., & Nicholas, A. P. (1993). A multi-parameter approach to fingerprinting suspended-sediment sources. In N. E. Peters, E. Hoehn, C. Leibundgut, N. Tase, & D. E. Walling (Eds.), *Tracers in hydrology* (pp. 329–338). Wallingford, UK: IAHS Press.
- Wilkinson, S. N., Hancock, G. J., Bartley, R., Hawdon, A. A., & Keen, R. J. (2013). Using sediment tracing to assess processes and spatial patterns of erosion in grazed rangelands, Burdekin River basin, Australia. *Agriculture, Ecosystems & Environment*, *180*, 90–102.
- Wilkinson, S. N., Olley, J. M., Furuichi, T., Burton, J., & Kinsey-Henderson, A. E. (2015). Sediment source tracing with stratified sampling and weightings based on spatial gradients in soil erosion. *Journal of Soils and Sediments*, *15*(10), 2038–2051.
- Zhang, X. C., Friedrich, J. M., Nearing, M. A., & Norton, L. D. (2001). Potential use of rare earth oxides as tracers for soil erosion and aggregation studies. *Soil Science Society of America Journal*, *65*, 1508–1515.
- Zhang, X. C., & Liu, B. L. (2016). Using multiple composite fingerprints to quantify fine sediment source contributions: A new direction. *Geoderma*, *268*, 108–118.